A proteoliposome-based system reveals how lipids control photosynthetic light harvesting

Received for publication, October 30, 2019, and in revised form, January 9, 2020 Published, Papers in Press, January 12, 2020, DOI 10.1074/jbc.RA119.011707

Stefanie Tietz[‡1], **Michelle Leuenberger**[§¶], **Ricarda Höhner**[‡2], **Alice H. Olson**[‡], **Graham R. Fleming**[§¶], and **Helmut Kirchhoff**[‡3]

From the [‡]*Institute of Biological Chemistry, Washington State University, Pullman, Washington 99164–6340,* [§]*Department of Chemistry, University of California, Berkeley, California 94720, and* [¶]*Molecular Biophysics and Integrated Bioimaging Division, Lawrence Berkeley National Laboratory, Berkeley, California 94720*

Edited by Joseph M. Jez

Integral membrane proteins are exposed to a complex and dynamic lipid environment modulated by nonbilayer lipids that can influence protein functions by lipid-protein interactions. The nonbilayer lipid monogalactosyldiacylglycerol (MGDG) is the most abundant lipid in plant photosynthetic thylakoid membranes, but its impact on the functionality of energy-converting membrane protein complexes is unknown. Here, we optimized a detergent-based reconstitution protocol to develop a proteoliposome technique that incorporates the major light-harvesting complex II (LHCII) into compositionally well-defined large unilamellar lipid bilayer vesicles to study the impact of MGDG on light harvesting by LHCII. Using steady-state fluorescence spectroscopy, CD spectroscopy, and time-correlated single-photon counting, we found that both chlorophyll fluorescence quantum yields and fluorescence lifetimes clearly indicate that the presence of MGDG in lipid bilayers switches LHCII from a light-harvesting to a more energy-quenching mode that dissipates harvested light into heat. It is hypothesized that in the *in vitro* system developed here, MGDG controls light harvesting of LHCII by modulating the hydrostatic lateral membrane pressure profile in the lipid bilayer sensed by LHCII-bound peripheral pigments.

Photosynthetic energy transformation starts with the harnessing of solar photons and the spatial transfer of the collected light energy to photochemically active reaction centers localized within photosystems (PS)[4] to ignite electron transport. The processes of light harvesting and energy transfer are realized by specialized light-harvesting pigment protein complexes (LHC, 1). LHCs were tuned by evolution for an almost loss-free ultrafast electronic excitation energy transfer between protein-anchored pigments (1, 2). Some LHCs are not only perfect light harvesters, but in addition have the remarkable built-in capacity to switch from a light-harvesting mode to an efficient energy-quenching mode under light stress (3–5). This energy-quenching mode (qE) is one of the most important photoprotective mechanisms in photosynthetic organisms ensuring survival and fitness in a highly dynamic environment (6). In plants and algae, LHCs fulfill their dual role as light harvester and energy quencher as transmembrane integral protein complexes buried in the amphiphilic thylakoid membrane system. Excellent structural data for the major plant LHCII exists that makes it an interesting candidate to study light harvesting in thylakoid membranes (7, 8). LHCII serves as the main light-harvesting antenna for PSII and under some conditions for PSI. Detailed structural information combined with data from ultra-fast and steady-state spectroscopy leads to an in-depth understanding of the functionality of the isolated LHCII and its dynamic switch between light harvesting and qE (*e.g.* 9–11). In native membranes, however, LHCII is embedded in a lipid bilayer. A substantial gap in our knowledge base exists on how the lipid matrix in thylakoid membranes interacts with LHCII (and other proteins) and modulates light harvesting. For nonphotosynthetic membrane protein complexes, like mechanosensitive channels and membrane transporters, strong evidence exists that the composition and physicochemical properties of the lipid bilayer have significant impact on the conformation and functionality of these proteins (12–17). A concept that bridges physicochemical lipid bilayer properties with structural and functional alterations of membrane proteins is the lateral membrane pressure (LMP) hypothesis (12, 18) also known as force-from-lipid principle (17). The so-called nonbilayer lipids play a central role in the LMP hypothesis. In contrast to bilayer-forming lipids that have an overall cylindrical shape, nonbilayer lip-

This work was supported by National Science Foundation Grant MCB-1616982; U.S. Department of Energy Grant DE-SC 0017160; and U.S. Department of Agriculture, National Institute of Food and Agriculture Hatch Projects 1005351 and 0119 (to H. K.). This work was also supported by the Director, Office of Science, Office of Basic Energy Sciences, of the U.S. Department of Energy under Contract DE-AC02–05CH11231 and the Division of Chemical Sciences, Geosciences, and Biosciences, Office of Basic Energy Sciences of the U.S. Department of Energy Grants DE-AC03–76SF000098 and FWP 449B (to G. R. F). The authors declare that they have no conflicts of interest with the contents of this article.

[1] Present address: Michigan State University–Dept. of Energy Plant Research Laboratory, MI State University, East Lansing, MI 48824.

[2] Present address: School of Biological Sciences, WA State University, P.O. Box 644236, Pullman, WA 99164.

[3] To whom correspondence should be addressed: P.O. Box 646340, Pullman, WA 99164–6340. Tel.: 1-509-335-3304; Fax: 1-509-335-7643; E-mail: kirchhh@wsu.edu.

[4] The abbreviations used are: PS, photosystems; LHC, light-harvesting complex; qE, energy-quenching mode; LMP, lateral membrane pressure; HII, inverted hexagonal; LUV, large unilamellar vesicles; chl, chlorophyll; Abs, absorption value; TCSPC, time-correlated single photon counting; neo, neoxanthin; zea, zeaxanthin; F655, fluorescence at 655nm.

Downloaded from http://www.jbc.org/ at Washington State University Libraries on March 24, 2020

ids adopt a conical shape because their hydrophilic head group is smaller than the hydrophobic fatty acid tail. According to the lipid shape-structure concept (19) isolated conical-shaped nonbilayer lipids adopt nonlamellar structures such as inverted hexagonal (HII) phases in aqueous environments (rods of aligned lipids with the smaller head groups facing to the center of the rod and the fatty acids moiety facing outward). Many biomembranes contain a high percentage of nonbilayer lipids. Thylakoid membranes are dominated by the nonbilayer lipid monogalactosyldiacylglycerol (MGDG) that makes up about half of the total lipids (20, 21). The role of MGDG in photosynthetic energy transformation and its regulation is not established and remains elusive (21). Recently, it was shown that the presence of MGDG in the lipid matrix increases the structural stability of LHCII. This observation was interpreted as a consequence of modulation of LMP by this nonbilayer lipid (22). Nonbilayer lipids generate a higher lateral membrane pressure in the hydrocarbon region of the lipid bilayer because of their bulkier fatty acid part requiring more space (12, 13, 18, 23). The higher membrane pressure in the hydrophobic membrane region is sensed by membrane proteins that can modulate their conformation and functionality (24). For photosynthetic thylakoid membranes, molecular dynamics simulation confirmed that the presence of MGDG leads to a significant increase of the physical pressure in the hydrophobic fatty acid part (25). In this study, the impact of the nonbilayer lipid MGDG for LHCII functionality was tested by reconstituting isolated trimeric LHCII from spinach into lipid liposomes with different mol % of MGDG leading to proteoliposomes. Proteoliposomes are a versatile tool for studying energy-transducing membrane proteins (26) and have frequently been used in photosynthesis research (*e.g.* 27–32). Here, a detergent-based reconstitution protocol (26, 32) was optimized which generated LHCII-proteoliposomes with a very low protein density, allowing specifically the study of lipid-protein interactions.

Results

LHCII proteoliposomes with low protein density

Most studies on LHCII proteoliposomes used relatively high protein-to-lipid ratios leading to LHCII aggregation. LHCII aggregation is known to cause energy quenching by changes of the conformation of the pigment-protein complex (*e.g.* 33–35). LHCII aggregation interferes with lipid-only–induced alterations of the LHCII structure and function. To avoid protein-protein interactions by LHCII aggregation, we refined a detergent-based reconstitution protocol leading to very low protein densities in the final LHCII-proteoliposomes (Fig. 1). Addition of detergent to preformed large unilamellar lipid vesicles (LUV) (made of isolate thylakoid lipids) destabilizes the LUV bilayer necessary to allow LHCII incorporation (*step II* in Fig. 1*A*). LHCII was isolated from spinach. We used the detergent Triton X-100 for the LUV destabilization because it has a distinct absorption peak around 275 nm (Fig. 1*A*, *bottom*) that is missing for other detergents. The 275-nm Triton X-100 absorption peak is used to monitor detergent removal upon Bio-Bead treatment (Fig. 1*A*, *bottom*). Thus, it is ensured that the final LHCII proteoliposomes are detergent free. The successful incorporation of LHCII into the liposomes is validated by colocalization of fluorescent dyes (Fig. S1) that stain the lumen of the proteoliposomes (pyranine), the lipid bilayer (BODIPY), and LHCII (chlorophyll autofluorescence). The final proteoliposomes have a mean diameter of about 200 nm (Fig. 1*B*), determined by dynamic light scattering and a molar lipid-to-trimeric LHCII ratio of about 60,000 (Fig. 1*C*). Assuming that lipids are organized in a bilayer and occupy on average a molecular area of 0.66 nm^2 (36) and assuming that each LHCII trimer binds 42 chl (7, 8), it follows that each proteoliposome contains on average six LHCII trimers. This translates to a protein area fraction of smaller than 0.2% (area of trimeric LHCII is 33.2 nm^2), *i.e.* the LHCII concentration in proteoliposomes is very diluted. Two types of proteoliposomes were prepared to study the impact of MGDG on the LHCII functionality. One type contained MGDG and the other type contained almost no MGDG (small traces come as contamination from other thylakoid lipids). For the latter, MGDG was replaced by the charge-neutral DGDG. The lipid and fatty acid analysis measured for the final LHCII-proteoliposomes preparation is given in Fig. 1*D*. The fatty acid profile for the four thylakoid lipid classes is in accordance with the literature (37). Native thylakoid membranes contain about 50 mol % MGDG (20, 21). We decided to produce proteoliposomes with no more than 25 mol % MGDG (Fig. 1*D*) because some reports mentioned that higher MGDG abundances in liposomes can lead to HII formation (22, 38). Although it is debated whether high MGDG concentration leads to HII phase in liposomes we want to avoid nonbilayer HII formation in LHCII proteoliposomes, and as a consequence the MGDG concentration was reduced to a "safe" value.

Structural integrity of LHCII in proteoliposomes

The structural integrity and protein aggregation level of LHCII in proteoliposomes was probed by fluorescence spectroscopy and circular dichroism (CD). Room temperature chlorophyll (chl) fluorescence spectra preferentially exciting chl a at 420 nm or chl b at 475 nm (39) reveal similar values for the maximal fluorescence emission wavelengths (Fig. S2, *A* and *B*). This indicates efficient energy transfer from chl b to chl a in LHCII proteoliposomes. This is further supported by almost indistinguishable normalized chl fluorescence emission spectra if exited at 420 nm or 475 nm for both MGDG-containing and MGDG-depleted proteoliposomes (Fig. S2, *C* and *D*). The presence of excitonically disconnected chl b would lead to a blue-shifted shoulder for 475 nm excitation compared with 420 nm excitation. The lack of this shoulder gives clear evidence that all chl b is energetically well-connected to the LHCII pigment system. Low temperature (77 K) fluorescence spectra (Fig. 2*A*) provide information about the unbinding of chls and LHCII aggregation. Diagnostic for chl b unbinding is an emission at around 655 nm (preferential chl b excitation at 475 nm). 77 K emission spectra of both proteoliposomes with and without MGDG reveal a very small 655 nm signal, indicating that the vast majority of LHCII in proteoliposomes is intact (Fig. 2*A*), which is in agreement with the data in Fig. S2. Additionally, there is no difference in the 655 nm (F655) peak between MGDG-containing and MGDG-depleted LHCII proteoliposomes (see *error bars* in Fig. 2*A*). Furthermore, the emission

Downloaded from http://www.jbc.org/ at Washington State University Libraries on March 24, 2020

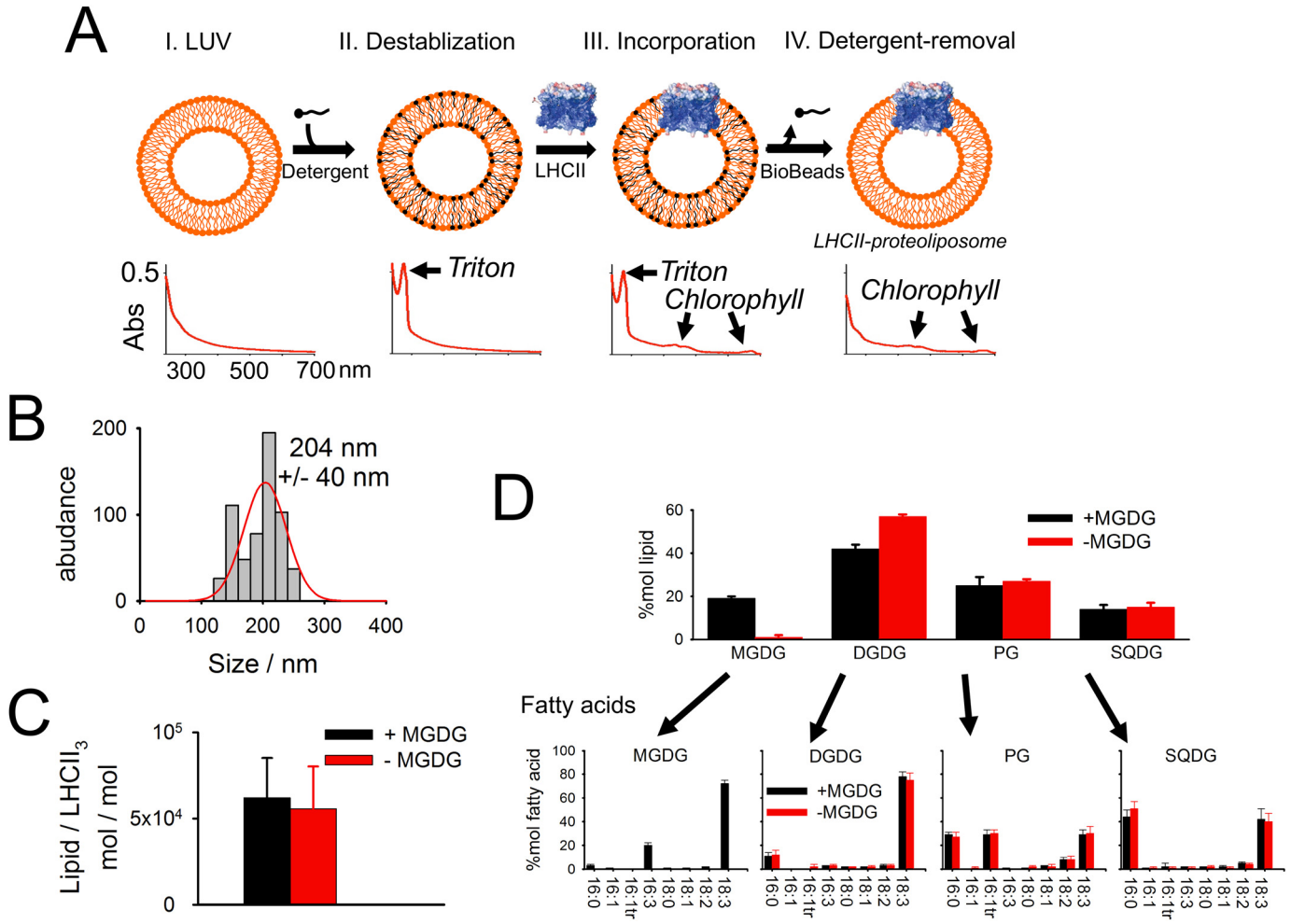

Figure 1. Establishing an LHCII-proteoliposome system. *A*, scheme of producing LHCII proteoliposomes from LUVs by the detergent-mediated incorporation approach (see text for details). Graphs at the bottom shows absorption spectra at the different preparation steps. Note the Triton X-100 peak at 275 nm that disappears after Bio-Beads treatment. *B*, proteoliposomes size determination by dynamic light scattering. The ± gives half of the full width at half-maximum ($n = 5$, biological repetitions). No difference was apparent between +MGDG and −MGDG proteoliposomes. *C*, molar lipid to trimeric LHCII ratio in proteoliposomes. Lipid content was determined from 2D TLC, LHCII trimer content from chl determination assuming 42 chls per trimer. *Error bars* represent 95% confidence interval ($n = 5$, biological repetitions). *D*, lipid and fatty acid analysis. *Upper panel* shows the mol % for the four different lipid classes in +MGDG and −MGDG proteoliposomes measured by 2D TLC. *Error bars* represent S.D. ($n = 3$, biological repetitions for both +MGDG and −MGDG samples). Fatty acids for the individual lipid classes separated by TLC were quantified by GC. *Error bars* represent S.D. ($n = 4$ for +MGDG and $n = 3$ for −MGDG proteoliposomes).

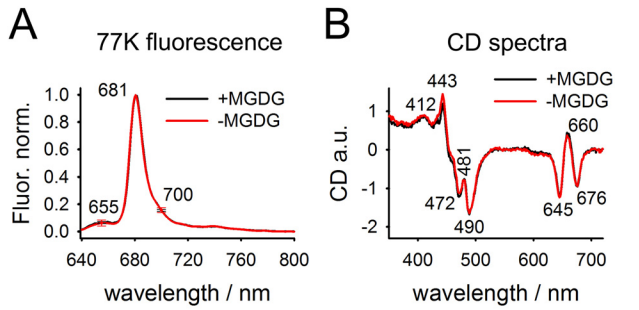

Figure 2. Spectroscopic characterization of LHCII-proteoliposomes. *A*, representative chl fluorescence spectra of +MGDG and −MGDG proteoliposomes. Note the low emissions at 655 nm (indicative for chl b) and 700 nm (indicative for LHCII aggregates). *Error bars* at both wavelengths represent S.D. from 13 biological repetitions. *B*, room temperature CD spectra. The spectra show the mean of two biological replicates per sample type. A CD spectrum for the pure buffer was subtracted. Characteristic wavelength for LHCII trimer and protein aggregation are indicated (see text for details).

around 700 nm (F700) is a signature for LHCII aggregation (33, 40, 41). F700 emission for detergent-solubilized LHCII trimers is about 10% relative to the maximal emission at around 681 nm (F681) (41). An increase in the F700/F681 ratio reflects LHCII-trimer aggregation. In LHCII proteoliposomes the F700/F681 ratio is 15–16% (Fig. 2*A*). This low F700/F681 ratio in LHCII proteoliposomes suggests a very low level of LHCII-trimer aggregation, as expected for highly protein-diluted membranes. A low level of LHCII aggregation is also supported by fluorescence lifetime measurements (see below). As for the 655 nm emission, no statistically significant difference of the F700/F681 ratio exists between proteoliposomes with and without MGDG (see *error bars* in Fig. 2*A*). These conclusions are supported and complemented by CD spectra of LHCII-proteoliposomes. The CD spectra in the Soret region show a pronounced negative peak at 472 nm ((−)472 nm) that is characteristic for trimeric LHCII and is absent in monomeric LHCII (42–44). In detail, the (−)472 nm to (−)490 nm ratio in trimeric LHCII is between 0.7

Downloaded from http://www.jbc.org/ at Washington State University Libraries on March 24, 2020

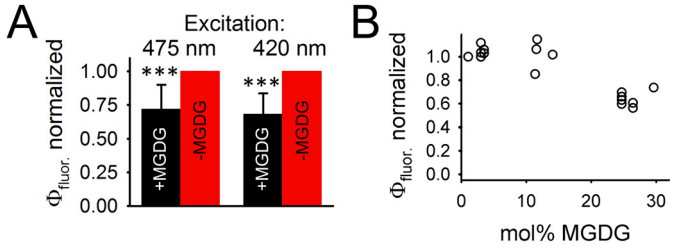

Figure 3. Quantum yields in fluorescence emission (Φ_{fluor}). *A*, comparison of Φ_{fluor} for +MGDG and −MGDG proteoliposomes measured for 475 nm and 420 nm excitation (*indicated*). The data were measured on pairs of +MGDG and −MGDG proteoliposomes prepared at the same day. Φ_{fluor} for +MGDG was normalized to the same day −MGDG counterpart (set to 1). Data are from 11 pairs. *Error bars* represent S.D. and ***, indicates *p* value of <0.001 (Student's *t* test). The mol % of the +MGDG samples is about 20%. *B*, dependence of mol % MGDG in proteoliposomes on Φ_{fluor}. The mol % of MGDG was determined by TLC.

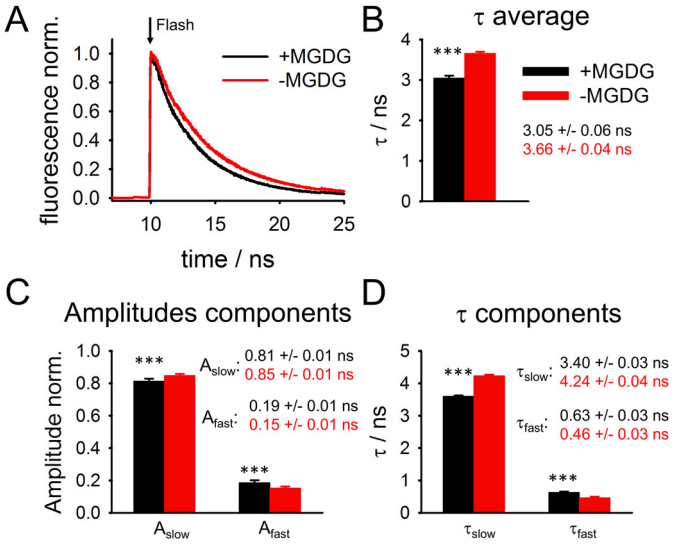

Figure 4. TCSPC of chl fluorescence on LHCII proteoliposomes. *A*, representative examples of fluorescence relaxation kinetics after laser excitation (*flash*). *B*, relaxation kinetics were fitted with two exponentials. The average fluorescence lifetime τ_{av} was calculated from the amplitude-weighted single exponential lifetimes. *C* and *D*, amplitudes (*C*) and lifetimes (*D*) for the slow and fast fluorescence relaxation components. *Error bars* represent S.D. ($n = 7$ for +MGDG and $n = 10$ for −MGDG proteoliposomes). ***, indicates *p* value of <0.001 (Student's *t* test).

and 0.75 (43, 44), that is very similar to the ratio of 0.72 in our LHCII proteoliposomes (Fig. 2*B*). Further support for a trimeric LHCII organization in proteoliposomes is given by the broad (+)412 nm signal (Fig. 2*B*) that is absent in LHCII monomers (42). Clear signatures for LHCII aggregation are the occurrence of a (−)438 nm peak and a significant reduced (−)676 nm peak (45). Absence of these signatures in CD spectra of the LHCII proteoliposomes (Fig. 2*B*) indicate that LHCII is in a nonaggregated state, which is in line with the low F700/F681 ratio (see above). There are also no significant differences in CD spectra in MGDG-containing and MGDG-depleted proteoliposomes. Overall, the fluorescence and CD spectra demonstrate the structural integrity of LHCII in our proteoliposomes and its organization as a nonaggregated trimer.

Impact of MGDG on the LHCII fluorescence yield

A straightforward method for detecting energy quenching in isolated LHCII is the measurement of the relative chl fluorescence yield (Φ_{fluor}) because a decrease in Φ_{fluor} gives strong indication for an increased dissipative deactivation of electronic excited states into heat. Φ_{fluor} of the various samples can be compared by normalizing the maximal fluorescence intensity by the absorbance of each sample at the excitation wavelength. This fluorescence-to-absorption ratio (Φ_{fluor}) quantifies the amount of light emitted from LHCII per light absorbed by the pigment protein complex. Excitation wavelengths probing either preferentially chl a (420 nm) or chl b (475 nm) were used (Fig. S2). To determine the absorption values at 420 nm (Abs_{420}) and 475 nm (Abs_{475}), the spectra were baseline corrected for an unspecific light-scattering background (continuous increase from red to blue spectral regions) caused by the proteoliposomes (Fig. S2*E*). Room temperature fluorescence excited at either 420 nm (Fig. S2*A*) or 475 nm (Fig. S2*B*) was measured from the same samples used for absorption spectroscopy allowing Φ_{fluor} calculation. To compare MGDG-containing and MGDG-depleted proteoliposomes the Φ_{fluor} for −MGDG proteoliposomes were set to 1 (Fig. 3). It turns out that Φ_{fluor} for LHCII in MGDG-containing proteoliposomes is about 25% lower compared with their MGDG-depleted counterparts. This result provides strong evidence that the presence of MGDG in lipid bilayers causes energy quenching in trimeric LHCII. To study the impact of MGDG on energy quenching in LHCII in more detail a third MGDG concentration was added at around 10 mol % MGDG (Fig. 3*B*). Φ_{fluor} in LHCII proteoliposomes with about 10 mol % MGDG is very similar to Φ_{fluor} in MGDG-depleted samples.

Chl fluorescence lifetime analysis of LHCII proteoliposomes

A more in-depth characterization of MGDG-dependent energy quenching in LHCII was performed by measuring chl fluorescence lifetimes in +MGDG and −MGDG proteoliposomes by time-correlated single photon counting (TCSPC) (Fig. 4). Fig. 4*A* gives examples for chl fluorescence relaxation kinetics for +MGDG and −MGDG LHCII proteoliposomes. Kinetics for +MGDG proteoliposomes are clearly faster than in MGDG-depleted samples, suggesting that MGDG causes shortening of the excited state lifetime in LHCII. For both types of proteoliposomes the fluorescence relaxation kinetics can be fitted by bi-exponential decay curves as is typical for isolated trimeric LHCII (28, 46–48). It was confirmed that the bi-exponential parameters derived from TCSPC analysis are independent on the laser power used for this experiment (Fig. S3), indicating absence of exciton-exciton annihilation events. The average fluorescence lifetime (τ_{av}) for MGDG-depleted proteoliposomes calculated from a bi-exponential fit is 3.66 ns (Fig. 4*B*). This lifetime is in agreement with literature values for nonaggregated trimeric LHCII in detergent shells that are around 3.6 ns (28, 35, 40, 47). The good correlation of average fluorescence lifetimes between LHCII in detergent and LHCII in MGDG-depleted proteoliposomes indicates that LHCII is in a non–energy-quenched light-harvesting state in the latter. Closer inspection of the LHCII fluorescence kinetics in MGDG-depleted proteoliposomes reveals that the faster exponential component has a time constant of $\tau_{fast} = 0.46$ ns with a relative amplitude (A) of $A_{fast} = 0.15$ (Fig. 4). For the slower

Downloaded from http://www.jbc.org/ at Washington State University Libraries on March 24, 2020

dominating component (A_{slow} = 0.85) τ_{slow} is 4.24 ns. It is noteworthy that the τ_{fast} (~0.5 ns) component is most likely not caused by LHCII aggregation (48). Rather it was hypothesized that the slow and fast fluorescence lifetimes reflect two conformations of nonaggregated LHCII trimers (48). No indication was found for a component with very long lifetimes that would indicate free chls, which have fluorescence lifetimes of around 6 ns (46, 48, 49). For example, chls that unbind from LHCII trimers by high Triton X-100 concentrations show lifetimes of about 5.8 ns (46, 48). The absence of these very long–living decay components supports the conclusion that LHCII in proteoliposomes is structurally intact (see above). Addition of ~25 mol % MGDG to LHCII proteoliposomes induces significant changes in all four bi-exponential fluorescence relaxation parameters (Fig. 4, *C* and *D*). In detail, A_{fast} increases slightly by ~4% at the expense of A_{slow}. At the same time τ_{slow} (3.4 ns) is ~20% faster and τ_{fast} (0.63 ns) ~37% slower in MGDG-containing LHCII-proteoliposomes. As a consequence of these alterations in the two exponential fluorescence decay phases in +MGDG proteoliposomes the average lifetime (τ_{av}) of LHCII decreased by 17% (3.05 ns) relative to their −MGDG counterparts (Fig. 4*B*). If the decrease of the steady state chl fluorescence yield (Φ_{fluor}) (Fig. 3*A*) is exclusively caused by shortening of fluorescence lifetimes (activation of energy dissipative pathways in LHCII) then it is expected that the MGDG-induced decrease in τ_{av} and the corresponding decreases in Φ_{fluor} have the same magnitude. The MGDG-induced decrease in Φ_{fluor} seems slightly higher with ~25%. However, it must be pointed out that this difference between τ_{av} and Φ_{fluor} is statistically not significant (see *error bar* in Fig. 3*A*). It follows that the decline in fluorescence yield of LHCII in +MGDG liposomes could be entirely explained by a shortening of fluorescence lifetimes.

Discussion

For nonphotosynthetic membranes, there is good evidence that generic physicochemical properties of lipid bilayers modulated by nonbilayer lipids exert control over membrane protein conformation and function. Until today the role of the nonbilayer thylakoid lipid MGDG on photosynthetic light harvesting was unknown. This study employed proteoliposomes to study the role of MGDG on the structure and function of plant LHCII. The benefit of proteoliposomes is that they are compositionally and structurally well-defined, *i.e.* they offer a significant advantage over complex structured intact thylakoid membranes for identification of cause and effect relationships. A prerequisite to examine lipid-induced alterations on LHCII structure and function with proteoliposomes is avoidance of LHCII aggregation by a drastic dilution in protein density. To our knowledge, only two publications published studies on LHCII on highly protein-diluted proteoliposomes. However, in both publications severe problems were reported for highly protein-diluted samples. In Ref. 30, LHCII trimers monomerized, and in Ref. 31, proteoliposomes without MGDG form mixtures of lipid vesicles and planar sheets, making the direct comparison with their MGDG-containing counterparts difficult. Here we established a LHCII proteoliposome reconstitution protocol with very low protein densities (molar lipid/LHCII trimer ratio ~60,000) embedded in large (~200 nm diameter) LUVs with different mol % of MGDG. The large proteoliposome diameter ensures minimized membrane bending forces for LHCII in the lipid bilayer. In detail, the curvature of a proteoliposome with 200 nm diameter leads to height difference of the lipid bilayer on two opposite sides of the LHCII trimer (distance 7.5 nm) of less than three Å, *i.e.* LHCII experience an almost flat lipid-membrane that resembles the situation in native thylakoid membranes. Steady state fluorescence, CD spectroscopic, and fluorescence lifetime analyses of LHCII for both MGDG-depleted and MGDG-containing proteoliposomes (Fig. 2) reveal the structural integrity of the complex (no chl unbinding) as well as its organization as a nonaggregated trimer, laying the foundation to study lipid-LHCII interactions specifically. The key outcome of this study is that presence of MGDG in proteoliposomes leads to significant energy quenching of LHCII (Φ_{fluor} is lower and τ_{av} is shorter) (Figs. 3 and 4). Because nothing else changed in the two types of proteoliposomes except the MGDG content (*i.e.* both −MGDG and +MGDG proteoliposomes contain the same amount of charged lipids, Fig. 1*D*) this result gives strong evidence for the specific role of the nonbilayer MGDG for modulating light harvesting by LHCII, *i.e.* MGDG in lipid bilayers induces energy quenching in LHCII. However, it is noteworthy that the MGDG-induced change in fluorescence lifetimes from 3.66 to 3.05 ns is a magnitude higher than the photochemical trapping time in PSII (300 to 500 ps), *i.e.* the impact on competing with photochemistry is small. On the other hand, we want to point out that native thylakoid membranes contain about ~50 mol % MGDG thus the fluorescence quenching observed here with ~20 mol % could be significantly higher in native thylakoid membranes.

An intriguing question is the molecular mechanism of how nonbilayer MGDG determines the light-harvesting efficiency of LHCII. One possibility is that modulation of the LMP by MGDG leads to conformational changes in LHCII that trigger dissipative pathways for excited pigment states. To explore this possibility in more detail we generated an in-scale model of the LHCII trimer together with LMP changes induced by MGDG derived from molecular dynamics simulations (25) (Fig. 5). Fig. 5 gives the false color-coded structural flexibility of LHCII that is derived from the crystallographic temperature (or B) factor (8). The color code varies from very rigid regions (*blue*) to highly flexible regions (*red*). As expected for a membrane integral protein complex the hydrophobic part made of rigid α-helices embedded in the lipid bilayer is mostly very stiff (8, 50, 51). However, an important exception is the xanthophyll neoxanthin (neo) that protrudes from the protein surface into the fatty acid region of the lipid bilayer. This neo is highly flexible (8, 51). Comparing MGDG-induced lateral pressure changes along the *z* axis of the lipid bilayer (*red curve* in Fig. 5, *bottom*) with the LHCII flexibility reveals a significant (several 10 MPa) increase in lipid-bilayer pressure on the level of neo (*orange arrow*). Thus, it is likely that the presence of MGDG in lipid bilayers leads to bending of LHCII-bound neo as was reported for LHCII crystals where adjacent LHCII proteins cause neo bending (34). Interestingly, based on the fact that neo distortion correlates with energy dissipation (51–53), it was hypothesized that the bending of LHCII-bound neo switches the protein

Downloaded from http://www.jbc.org/ at Washington State University Libraries on March 24, 2020

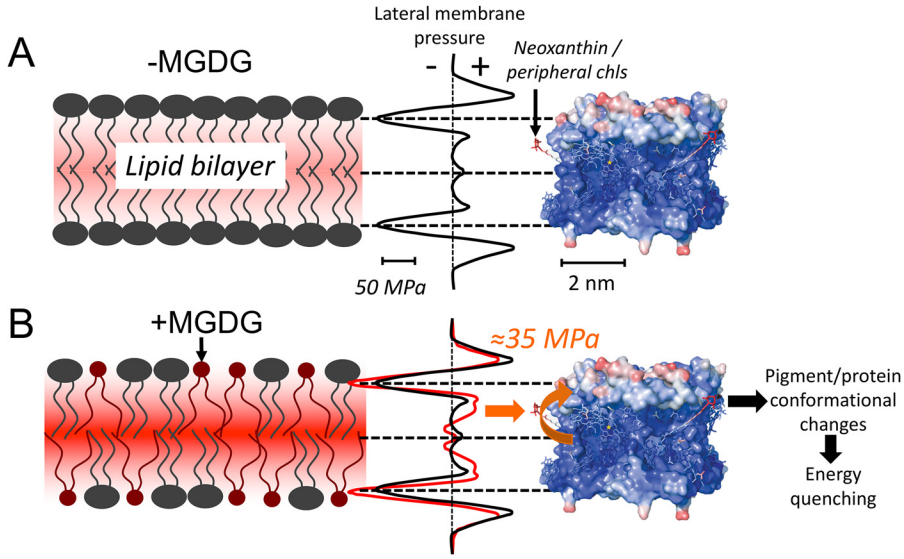

Figure 5. In scale model of the LMP profile and the LHCII trimer structure for membranes with only bilayer forming lipids. *A* and *B*, DOPC (*A*) and membranes with nonbilayer MGDG (*B*). The LMP profiles were taken from Ref. 25. The temperature-factor representation of the LHCII trimer structure is from Ref. 8 and is a measure of the flexibility of the protein (*blue*, rigid; *red*, flexible). The position of neo (*A*) and the MGDG-induced increase in pressure in the fatty acid region (*B*, *orange arrow*) are indicated. See text for additional details.

from a light harvester to an energy dissipater (52, 54). Indeed, molecular dynamics simulation identified a strong correlation between neo bending, pigment rearrangement in LHCII, and energy quenching (51). However, it is also possible that neo distortion is not the trigger but only a reporter for an energy dissipative state that is established by other pigment-pigment rearrangements (*e.g.* Chl a603-lutein2) (51). Also, chls a611/612 are potential candidates for LMP-induced quenching because they are localized at the LHCII periphery (PDB ID: 1RWT). We speculate that the lateral pressure increase at a certain *z*-position in the lipid bilayer, caused by MGDG, leads to distortion of neo or other pigment-pigment rearrangements and switches LHCII to an energy-quenching state (Fig. 5, *bottom*). A direct impact of physical pressure on light harvesting by LHCII was observed by studying the functionality of the isolated detergent-solubilized protein at different isotropic hydrostatic pressures measured with a high-pressure cell (48). In accordance with our study, τ_{av} and Φ_{fluor} decrease with an increase in hydrostatic pressure in the pressure cell, *i.e.* LHCII switches to an energy-quenched mode (48). The similarities in both studies goes further: In Ref. 48, the amplitudes of the two fluorescence lifetime components change with increasing pressure, *i.e.* A_{slow}/A_{fast} decreases. The same tendency is observed for +MGDG liposomes. A_{slow}/A_{fast} decreases from 5.6 in MGDG-depleted proteoliposomes to 4.4 in MGDG-containing samples (Fig. 4*C*). Furthermore, in the isotropic pressure cell experiment τ_{slow} accelerates, whereas τ_{fast} decelerates with higher pressure (48). We observed the same changes from −MGDG to +MGDG proteoliposomes (Fig. 4*D*). These similarities between isotropic hydrostatic pressure experiments on detergent-solubilized LHCII trimers and the impact of MGDG in LHCII proteoliposomes support the model that the MGDG-dependent pressure increases in hydrophobic regions of the lipid bilayer are sensed by flexible LHCII parts leading to energy quenching (Fig. 5). An intriguing outcome of the study of Ref. 48 is that pressure-induced energy quenching is caused by very localized and small conformational changes and not by large-scale compression of the overall protein. These localized structural changes explicitly include the possibility of neo bending (48) in support of our model presented in Fig. 5.

The physiological relevance for a LMP-dependent mechanism to switch LHCII structure and function as proposed here is given if the LMP is variable, *i.e.* the LMP can be changed by environmental factors. Three observations indeed indicate that LMP in thylakoid is variable. (i) Under certain conditions MGDG separates to nonbilayer HII phases in intact thylakoid membranes (*e.g.* 55–58). This lipid-phase separation of MGDG would decrease the abundance of MGDG in the bilayer phase. As a consequence, the lateral membrane pressure in hydrophobic membrane bilayer regions decreases that according to the model in Fig. 5 would switch LHCII to a light-harvesting state. Interestingly HII formation was found stimulated by low light treatment (58), *i.e.* at situations where efficient light harvesting is required and not photoprotection. (ii) The results summarized in (i) measured large-scale HII formation that are visible in electron micrographs. However, recent molecular dynamics simulations indicated that nonbilayer HII formation could be more frequent on a smaller nanometer-length scale that is not detectable by conventional EM (36) as was proposed earlier (56). The molecular dynamics study reveals that the propensity for HII formation is strongly dependent on environmental conditions (*e.g.* water content). (iii) The LMP profile is a generic physicochemical property of the lipid bilayer and is therefore dependent not only on nonbilayer lipids but on all lipophilic membrane components. In this respect, the xanthophyll zeaxanthin (zea) is interesting. The presence of zea in the lipid bilayer increases membrane order and rigidity (59, 60) that is known to enhance the lateral membrane pressure in hydrophobic membrane regions (13). Zea is converted from violaxanthin by the xanthophyll cycle and promotes qE formation (61, 62). Thus, modulation of generic physicochemical membrane properties by free zea in the membrane could be another way to

Downloaded from http://www.jbc.org/ at Washington State University Libraries on March 24, 2020

control LMP and therefore light harvesting by LHCII. It follows that the xanthophyll cycle has two implications. First, zea would activate qE directly by the well-established binding to LHCIIs (61). Second, zea could modulate light harvesting indirectly via changes in LMP. The three examples presented above demonstrate that the lipid matrix in thylakoid membranes is dynamic and responsive to environmental conditions that could modulate the LMP that in turn could control light-harvesting efficiency by LHCII (Fig. 5). Furthermore, evidence exists that the lipid/fatty acid content in plant thylakoid membranes undergo diurnal alterations (63, 64) and change under stress like heat (65), cold (66), hypoxia (67), drought (68), and phosphate starvation (69). However, future studies have to reveal the dynamics of lipid/fatty acid compositions and its implications on light harvesting.

Experimental procedures

Isolation of trimeric LHCII

Trimeric LHCII was isolated from dark-adapted spinach from a local market according to Ref. 41. This protocol goes back to the original Triton X-100–based isolation procedure described in Refs. 70 and 71. The final LHCII preparation was solubilized in 0.37% Triton X-100 at a chl concentration of 1.65 mM.

Preparation of LHCII proteoliposomes

For liposomes, the isolated plant lipids MGDG (C36:6 and C34:6), DGDG (C36:6 and C34:3), PG (C34:4 and C34:3), and SQDG (C34:3) were used (Lipid Products). Approximately 5 μmol of isolated lipids in chloroform were mixed and evaporated off by nitrogen gas to form a thin lipid layer. The lipid film was rehydrated in a 10 mM HEPES buffer (pH 7.6, KOH) and vortexed thoroughly. The resulting multilamellar liposomes were passed sequentially through a 0.4 μm and 0.2 μm nucleopore membrane using a high-pressure extruder (Lipex™) at ~3.5 bar for the 0.4 μm extrusion, and 10 bar for the 0.2 μm extrusion, leading to LUVs. The lipid concentration in LUVs was determined by 2D thin layer chromatography (TLC) as described in Ref. 72. The lipid concentration in LUV stock was adjusted to 0.8 mM in 1.6 ml. Triton X-100 was added to a final concentration of 1 mM to destabilize the liposomes. After 5 min of incubation under slow stirring, 200 μl of isolated LHCII at a chl concentration of 25 μM (presolubilized in 600 μM Triton X-100/10 mM HEPES, pH 7.6) was added and incubated for 30 min at room temperature (incorporation of the protein into LUVs), the Triton X-100 was removed with 25 mg Bio-Beads™ SM-2 Resin overnight at 4 °C, followed by two 100-mg Bio-Beads™ addition steps for an hour and 45 min, respectively. The Triton removal was tracked using the 275 nm absorbance. Finally, proteoliposomes were further purified by gel filtration with a PD-10 Sephadex filtration column. Proteoliposomes were stored on ice in the dark and used freshly. The pigment composition of proteoliposomes with and without MGDG are (relative to total Chl): neoxanthin, 0.9 ± 0.1 and 1.0 ± 0.1; violaxanthin, 0.2 ± 0.1 and 0.3 ± 0.1; lutein 2.4 ± 0.1 and 2.3 ± 0.1, respectively. No zeaxanthin was detected.

Biochemical characterization

The lipid classes (MGDG, DGDG SQDG, PG) of proteoliposomes were quantified from lipid extracts by 2D TLC (73). From the same lipid extract fatty acids were converted to fatty acid methyl esters and quantified with gas chromatography (GC) by comparison of the fatty acid GC peaks with an internal fatty acid standard (2.613 nmol μl^{-1} 1,2,3-tripentadecanoyl-sn-glycerol, Nu-Chek Prep) as described in Ref. 65.

Steady-state fluorescence spectroscopy

For Φ_{fluor} measurements anaerobic conditions with undiluted proteoliposomes ($A_{420\ nm} = 0.1$) were established with a glucose/glucose-oxidase/catalase system. Oxygen measurements with a polarographic oxygen electrode reveal anaerobiosis after about 1 min with this enzyme system for about 1 h. Anerobiosis was required to minimize damage to LHCII because of the measuring lights (the lack of damage was indicated by unchanged signal amplitudes in repetitive measured fluorescence spectra). The same anaerobic sample was used for both absorption and fluorescence spectra to determine Abs_{420} and Abs_{475} and the maximum fluorescence intensities at these excitation wavelengths. Optical absorption spectra were recorded with a Hitachi U3900 spectrometer (2-nm slit width, 200–750 nm, optical path length 10 mm). Chl fluorescence spectra were measured with a FluoroMax 4 (Horiba Yvon) spectrofluorometer. Emission spectra between 640 to 800 nm (slit width 4 nm) were recorded for 420 or 475 nm excitation wavelength (slit width 2 nm). Fluorescence spectra at 77 K were measured with samples shock-frozen in liquid nitrogen. The excitation wavelength was set to 475 nm (2 nm slit width).

CD spectroscopy

VIS-CD (CD between 400 to 700 nm) spectroscopy measurements were performed with an AVIV 202SF CD spectrometer in a 0.5 cm cuvette in 10 mM HEPES/KOH buffer with concentrated proteoliposomes. The proteoliposomes concentration was performed with Amicon Ultra (30 kDa exclusion size). Redilution of concentrated proteoliposomes leads to no alteration in 77 K fluorescence spectra, indicating that the concentration did not changed LHCII integrity. Spectra recorded with HEPES buffer alone were subtracted. Measurements were done under anaerobic conditions (glucose/glucose-oxidase/catalase system).

Time correlated single photon counting

TCSPC measurements of fluorescence lifetime were acquired using Becker-Hickl module SPC-150 in conjunction with Becker-Hickl SPCM software. The 420-nm excitation pulses with a repetition rate of 3.8 MHz were generated by a Coherent Verdi G10 532 nm diode pumped laser which pumps a Coherent Mira 900f Ti:Sapphire Oscillator set to 840 nm. The resultant pulsed beam was then frequency doubled using a β-barium borate crystal to obtain 420-nm pulses at a repetition rate of 76 MHz. A pulse picker composed of a Harris SiO_2 crystal, and a Coherent 7200 cavity dumper in combination with an ENI voltage amplifier (model 403LA) to drive the acoustic waves was used to reduce the repetition rate to the desired 3.8 MHz for these experiments. Samples were prepared to have an optical

Downloaded from http://www.jbc.org/ at Washington State University Libraries on March 24, 2020

density of ~0.1 and measured in a Starna cell cuvette at room temperature with Spectrosil far UV Quartz windows, a 1-mm path length (front face detection), and a 0.4 ml volume. To obtain sufficient fluorescence counts from the sample, a long pass filter (polarizer set to magic angle) was used to detect wavelengths longer than 650 nm. 420-nm light was used to excite the chlorophyll a Soret band. Fluorescence was detected using a Hamamatsu R3809U microchannel plate photomultiplier tube (MCP PMT) and the IRF had a full width half-max of ~60 ps. Measurements were taken at several powers and it was determined that there was no power dependence for measurements taken at average powers less than 100 μW (Fig. S3). Therefore, all measurements taken at powers below 100 μW were averaged to obtain a larger sample size. The full width at half-maximum of the laser spot was about 650 μm. Under our conditions the fluorescence lifetimes were unchanged for at least 60 min indicating stability of the samples over the time of measurements.

Dynamic light scattering

The diameter of the LUVs and proteoliposomes was measured in a 10-mm cuvette using a Delsa™ Nano Zeta Potential and submicron particle size analyzer (BD Biosciences). Latex beads (BD Biosciences) between 100 nm and 300 nm in diameter were used to create a size standard curve. The liposome and proteoliposome diameters were determined from this standard curve.

Author contributions—S. T., M. L., R. H., and A. H. O. data curation; S. T., M. L., R. H., A. H. O., and H. K. formal analysis; S. T., R. H., A. H. O., and H. K. investigation; S. T., M. L., R. H., A. H. O., and H. K. methodology; R. H. and H. K. conceptualization; G. R. F. and H. K. funding acquisition; G. R. F. and H. K. writing-original draft; G. R. F. and H. K. writing-review and editing; H. K. supervision; H. K. project administration.

Acknowledgment—We thank Bart van Oort for help with TCSPC measurements and for many fruitful discussions.

References

1. Mirkovic, T., Ostroumov, E. E., Anna, J. M., van Grondelle, R., and Govindjee, Scholes, G. D. (2017) Light absorption and energy transfer in the antenna complexes of photosynthetic organisms. *Chem. Rev.* **117,** 249–293 CrossRef Medline
2. Croce, R., and van Amerongen, H. (2014) Natural strategies for photosynthetic light harvesting. *Nat. Chem. Biol.* **10,** 492–501 CrossRef Medline
3. Krüger, T. P., Wientjes, E., Croce, R., and van Grondelle, R. (2011) Conformational switching explains the intrinsic multifunctionality of plant light-harvesting complexes. *Proc. Natl. Acad. Sci. U.S.A.* **108,** 13516–13521 CrossRef Medline
4. Niyogi, K. K., and Truong, T. B. (2013) Evolution of flexible non-photochemical quenching mechanisms that regulate light harvesting in oxygenic photosynthesis. *Curr. Opin. Plant Biol.* **16,** 307–314 CrossRef Medline
5. Ruban, A. V. (2016) Nonphotochemical chlorophyll fluorescence quenching: Mechanism and effectiveness in protecting plants from photodamage. *Plant Physiol.* **170,** 1903–1916 CrossRef Medline
6. Külheim, C., Ågren, J., and Jansson, S. (2002) Rapid regulation of light harvesting and plant fitness in the field. *Science* **297,** 91–93 CrossRef Medline
7. Liu, Z., Yan, H., Wang, K., Kuang, T., Zhang, J., Gui, L., An, X., and Chang, W. (2004) Crystal structure of spinach major light-harvesting complex at 2.72-Å resolution. *Nature* **428,** 287–292 CrossRef Medline
8. Barros, T., Royant, A., Standfuss, J., Dreuw, A., and Kühlbrandt, W. (2009) Crystal structure of plant light-harvesting complex shows the active, energy-transmitting state. *EMBO J.* **28,** 298–306 CrossRef Medline
9. Müh, F., Madjet Mel-A., and Renger, T. (2010) Structure-based identification of energy sinks in plant light-harvesting complex II. *J. Phys. Chem. B.* **114,** 13517–13535 CrossRef Medline
10. Novoderezhkin, V., Marin, A., and van Grondelle, R. (2011) Intra- and inter-monomeric transfers in the light harvesting LHCII complex: The Redfield-Förster picture. *Phys. Chem. Chem. Phys.* **13,** 17093–17103 CrossRef Medline
11. Chmeliov, J., Gelzinis, A., Songaila, E., Augulis, R., Duffy, C. D., Ruban, A. V., and Valkunas, L. (2016) The nature of self-regulation in photosynthetic light-harvesting antenna. *Nat. Plants* **2,** 16045 CrossRef Medline
12. Cantor, R. S. (1997) Lateral pressure profiles in cell membranes: A mechanism for modulation of protein function. *J. Phys. Chem. B* **101,** 1723–1725 CrossRef
13. Gullingsrud, J., and Schulten, K. (2004) Lipid bilayer pressure profiles and mechanosensitive channel gating. *Biophys. J.* **86,** 3496–3509 CrossRef Medline
14. Karasawa, A., Swier, L. J., Stuart, M. C., Brouwers, J., Helms, B., and Poolman, B. (2013) Physicochemical factors controlling the activity and energy coupling of an ionic strength-gated ABC transporter. *J. Biol. Chem.* **288,** 29862–29871 CrossRef Medline
15. Phillips, R., Ursell, T., Wiggins, P., and Sens, P. (2009) Emerging roles for lipids in shaping membrane-protein function. *Nature* **459,** 379–385 CrossRef Medline
16. Khalili-Araghi, F., Gumbart, J., Wen, P.-C., Sotomayor, M., Tajkhorshid, E., and Schulten, K. (2009) Molecular dynamics simulations of membrane channels and transporters. *Curr. Opin. Struct. Biol.* **19,** 128–137 CrossRef Medline
17. Anishkin, A., Loukin, S. H., Teng, J., and Kung, C. (2014) Feeling the hidden mechanical forces in lipid bilayer is an original sense. *Proc. Natl. Acad. Sci. U.S.A.* **111,** 7898–7905 CrossRef Medline
18. van den Brinck-van der Laan, E., Killian, J. A., and de Kruijff, B. (2004) Nonbilayer lipids affect peripheral and integral membrane proteins via changes in the lateral pressure profile. *Biochim. Biophys. Acta* **1666,** 275–288 CrossRef Medline
19. Israelachvili, J. N., Marcelja, S., and Horn, R. G. (1980) Physical principles of membrane organization, *Q. Rev. Biophys.* **13,** 121–200 CrossRef Medline
20. Boudière, L., Michaud, M., Petroutsos, D., Rébeillé, F., Falconet, D., Bastien, O., Roy, S., Finazzi, G., Rolland, N., Jouhet, J., Block, M. A., and Maréchal, E. (2014) Glycerolipids in photosynthesis: Composition, synthesis and trafficking. *Biochim. Biophys. Acta* **1837,** 470–480 CrossRef Medline
21. Garab, G., Ughy, B., and Goss, R. (2016) Role of MGDG and non-bilayer lipid phases in the structure and dynamics of chloroplast thylakoid membranes. *Subcell Biochem.* **86,** 127–157 CrossRef Medline
22. Seiwert, D., Witt, H., Janshoff, A., and Paulsen, H. (2017) The non-bilayer lipid MGDG stabilizes the major light-harvesting complex (LHCII) against unfolding. *Sci. Rep.* **7,** 5158 CrossRef Medline
23. Orsi, M., and Essex, J. W. (2013) Physical properties of mixed bilayers containing lamellar and nonlamellar lipids: Insights from coarse-grain molecular dynamics simulations. *Faraday Discuss.* **161,** 249–272; discussion 273–303 CrossRef Medline
24. de Kruijff, B. (1997) Lipids beyond the bilayer. *Nature* **386,** 129–130 CrossRef Medline
25. Baczynski, K., Markiewicz, M., and Pasenkiewicz-Gierula, M. (2015) A computer model of a polyunsaturated monogalactolipid bilayer. *Biochimie* **118,** 129–140 CrossRef Medline
26. Rigaud, J. L., Pitard, B., and Levy, D. (1995) Reconstitution of membrane proteins into liposomes: Application to energy-transducing membrane proteins. *Biochim. Biophys. Acta* **1231,** 223–246 CrossRef Medline

Downloaded from http://www.jbc.org/ at Washington State University Libraries on March 24, 2020

ASBMB

27. McDonnel, A., and Staehelin, L. A. (1980) Adhesion between liposomes mediated by the chlorophyll a/b light-harvesting complex isolated from chloroplast membranes. *J. Cell Biol.* **84,** 40–56 CrossRef Medline
28. Moya, I., Silvestri, M., Vallon, O., Cinque, G., and Bassi, R. (2001) Time-resolved fluorescence analysis of the photosystem II antenna proteins in detergent micelles and liposomes. *Biochemistry* **40,** 12552–12661 CrossRef Medline
29. Yang, C., Boggasch, S., Haase, W., and Paulsen, H. (2006) Thermal stability of trimeric light-harvesting chlorophyll a/b (LHCIIb) in liposomes of thylakoid lipids. *Biochim. Biophys. Acta* **1757,** 1642–1648 CrossRef Medline
30. Natali, A., Gruber, J. M., Dietzel, L., Stuart, M. C. A., van Grondelle, R., and Croce, R. (2016) Light-harvesting complexes (LHCs) cluster spontaneously in membrane environment leading to shortening of their excited state lifetimes. *J. Biol. Chem.* **291,** 16730–16739 CrossRef Medline
31. Crisafi, E., and Pandit, A. (2017) Disentangling protein and lipid interactions that control a molecular switch in photosynthetic light harvesting. *Biochim. Biophys. Acta Biomembr.* **1859,** 40–47 CrossRef Medline
32. Rigaud, J. L., and Lévy, D. (2003) Reconstitution of membrane proteins into liposomes. *Methods Enzymol.* **372,** 65–86 CrossRef Medline
33. Horton, P., Ruban, A. V., Rees, D., Pascal, A. A., Noctor, G., and Young, A. J. (1991) Control of the light-harvesting function of chloroplast membranes by aggregation of the LHCII chlorophyll-protein complex. *FEBS Lett.* **292,** 1–4 CrossRef Medline
34. Pascal, A. A., Liu, Z., Broess, K., van Oort, B., van Amerongen, H., Wang, C., Horton, P., Robert, B., Chang, W., and Ruban, A. (2005) Molecular basis of photoprotection and control of photosynthetic light-harvesting. *Nature* **436,** 134–137 CrossRef Medline
35. Akhtar, P., Dorogi, M., Pawlak, K., Kovács, L., Bóta, A., Kiss, T., Garab, G., and Lambrev, P. H. (2015) Pigment interactions in light-harvesting complex II in different molecular environments. *J. Biol. Chem.* **290,** 4877–4886 CrossRef Medline
36. van Eerden, F. J., de Jong, D. H., de Vries, A. H., Wassenaar, T. A., and Marrink, S. J. (2015) Characterization of thylakoid lipid membranes from cyanobacteria and higher plants by molecular dynamics simulation. *Biochim. Biophys. Acta* **1848,** 1319–1330 CrossRef Medline
37. Joyard, J., Maréchal, E., Miège, C., and Block, M. A. (1998) Structure, distribution and biosynthesis of glycerolipids from higher plant chloroplasts. in: *Lipids in Photosynthesis: Structure Function and Genetics* (Siegenthaler, P.-A., and Murata, N., eds), pp. 21–52, Springer, Dordrecht, The Netherlands CrossRef
38. Sprague, S. G., and Staehelin, L. A. (1984) Effects of reconstitution method on the structural organization of isolated chloroplast membrane lipids. *Biochim. Biophys. Acta Biomembr.* **777,** 306–322 CrossRef
39. Croce, R., Cinque, G., Holzwarth, A. R., and Bassi, R. (2000) The Soret absorption properties of carotenoids and chlorophylls in antenna complexes of higher plants. *Photosyn. Res.* **64,** 221–231 CrossRef Medline
40. Pandit, A., Shirzad-Wasei, N., Wlodarczyk, L. M., van Roon, H., Boekema, E. J., Dekker, J. P., and de Grip, W. J. (2011) Assembly of the major light-harvesting complex II in lipid nanodiscs. *Biophys. J.* **101,** 2507–2515 CrossRef Medline
41. Kirchhoff, H., Hinz, H. J., and Rösgen, J. (2003) Aggregation and fluorescence quenching of chlorophyll a of the light-harvesting complex II from spinach in vitro. *Biochim. Biophys. Acta* **1606,** 105–116 CrossRef Medline
42. Hobe, S., Prytulla, S., Kühlbrandt, W., and Paulsen, H. (1994) Trimerization and crystallization of reconstituted light-harvesting chlorophyll a/b complex. *EMBO J.* **13,** 3423–3429 CrossRef Medline
43. Georgakopoulou, S., van der Zwan, G., Bassi, R., van Grondelle, R., and van Amerongen, H. (2007) Understanding the changes in the circular dichroism of light harvesting complex II upon varying its pigment composition and organization. *Biochemistry* **46,** 4745–4754 CrossRef Medline
44. Yang, C., Lambrev, P., Chen, Z., Jarvorfi, T., Kiss, A. Z., Paulsen, H., and Garab, G. (2008) The negatively charged amino acids in the lumenal loop influence the pigment binding and conformation of the major light-harvesting chlorophyll a/b complex of photosystem II. *Biochim. Biophys. Acta* **1777,** 1463–1470 CrossRef Medline
45. Ruban, A. V., Calkoen, F., Kwa, S. L. S., Grondelle R van, Horton, P., and Dekker, J. P. (1997) Characterisation of LHC II in the aggregated state by linear and circular dichroism spectroscopy. *Biochim. Biophys. Acta Bioenergetics* **1321,** 61–70 CrossRef
46. Ide, J. P., Klug, D. R., Kühlbrandt, W., Giorgi, L. B., and Porter, G. (1987) The state of detergent solubilized light-harvesting chlorophyll-*a/b* protein complex as monitored by picosecond time-resolved fluorescence and circular dichroism. *Biochim. Biophys. Acta Bioenergetics* **893,** 349–364 CrossRef
47. Palacios, M. A., Standfuss, J., Vengris, M., van Oort, B. F., van Stokkum, I. H., Kühlbrandt, W., van Amerongen, H., and van Grondelle, R. (2006) A comparison of the three isoforms of the light harvesting complex II using transient absorption and time-resolved fluorescence measurements. *Photosyn. Res.* **88,** 269–285 CrossRef Medline
48. van Oort, B., van Hoek, A., Ruban, A. V., and van Amerongen, H. (2007) Equilibrium between quenched and nonquenched conformations of the major plant light-harvesting complex studied with high-pressure time-resolved fluorescence. *J. Phys. Chem. B* **111,** 7631–7637 CrossRef Medline
49. Palacios, M. A., de Weerd, F. L., Ihalainen, J. A., van Grondelle, R., and van Amerongen, H. (2002) Superradiance and exciton (de)localization in light-harvesting complex II from green plants? *J. Phys. Chem. B* **106,** 5782–5787 CrossRef
50. Dockter, C., Müller, A. H., Dietz, C., Volkov, A., Polyhach, Y., Jeschke, G., and Paulsen, H. (2012) Rigid core and flexible terminus. *J. Biol. Chem.* **287,** 2915–2925 CrossRef Medline
51. Liguori, N., Periole, X., Marrink, S. J., and Croce, R. (2015) From light-harvesting to photoprotection: Structural basis of the dynamic switch of the major antenna complex of plants (LHCII). *Sci. Rep.* **5,** 15661 CrossRef Medline
52. Ruban, A. V., Berera, R., Ilioaia, C., van Stokkum, I. H., Kennis, J. T., Pascal, A. A., van Amerongen, H., Robert, B., Horton, P., and van Grondelle R. (2007) Identification of a mechanism of photoprotective energy dissipation in higher plants. *Nature* **450,** 575–578 CrossRef Medline
53. Haferkamp, S., Haase, W., Pascal, A. A., van Amerongen, H., and Kirchhoff, H. (2010) Efficient light-harvesting by photosystem II requires an optimized protein packing density in grana thylakoids. *J. Biol. Chem.* **285,** 17020–17028 CrossRef Medline
54. Ruban, A. V., Johnson, M. P., and Duffy, C. D. P. (2012) The photoprotective molecular switch in the photosystem II antenna. *Biochim. Biophys. Acta* **1817,** 167–181 CrossRef Medline
55. Webb, M. S., and Green, B. R. (1991) Biochemical and biophysical properties of thylakoid acyl lipids. *Biochim. Biophys. Acta Bioenergetics* **1060,** 133–158 CrossRef
56. Garab, G., Lohner, K., Laggner, P., and Farkas, T. (2000) Self-regulation of the lipid content of membranes by non-bilayer lipids: A hypothesis. *Trends Plant Sci.* **5,** 489–494 CrossRef Medline
57. Krumova, S. B., Dijkema, C., de Waard, P., Van As, H., Garab, G., van Amerongen, H. (2008) Phase behaviour of phosphatidylglycerol in spinach thylakoid membranes as revealed by 31P-NMR. *Biochim. Biophys. Acta* **1778,** 997–1003 CrossRef Medline
58. Kirchhoff, H., Haase, W., Wegner, S., Danielsson, R., Ackermann, R., and Albertsson, P. A. (2007) Low-light-induced formation of semicrystalline photosystem II arrays in higher plant chloroplasts. *Biochemistry* **46,** 11169–11176 CrossRef Medline
59. Gruszecki, W. I., and Strzałka, K. (2005) Carotenoids as modulators of lipid membrane physical properties. *Biochim. Biophys. Acta* **1740,** 108–115 CrossRef Medline
60. Azadi Chegeni, F., Perin, G., Sai Sankar Gupta, K. B., Simionato, D., Morosinotto, T., and Pandit, A. (2016) Protein and lipid dynamics in photosynthetic membranes investigated by in-situ solid-state NMR. *Biochim. Biophys. Acta* **1857,** 1849–1859 CrossRef Medline
61. Jahns, P., Latowski, D., and Strzalka, K. (2009) Mechanism and regulation of the violaxanthin cycle: The role of antenna proteins and membrane lipids. *Biochim. Biophys. Acta* **1787,** 3–14 CrossRef Medline
62. Park, S., Fischer, A. L., Steen, C. J., Iwai, M., Morris, J. M., Walla, P. J., Niyogi, K. K., and Fleming, G. R. (2018) Chlorophyll-carotenoid excitation energy transfer in high-light-exposed thylakoid membranes investigated by snapshot transient absorption spectroscopy. *J. Am. Chem. Soc.* **140,** 11965–11973 CrossRef Medline
63. Browse, J., Roughan, P. G., and Slack, C. R. (1981) Light control of fatty acid synthesis and diurnal fluctuations of fatty acid composition in leaves. *Biochem. J.* **196,** 347–354 CrossRef Medline

Downloaded from http://www.jbc.org/ at Washington State University Libraries on March 24, 2020

64. Maatta, S., Scheu, B., Roth, M. R., Tamura, P., Li, M., Williams, T. D., Wang, X., and Welti, R. (2012) Levels of *Arabidopsis thaliana* leaf phosphatidic acids, phosphatidylserines, and most trienoate-containing polar lipid molecular species increase during the dark period of the diurnal cycle. *Front. Plant Sci.* **3,** 49 CrossRef Medline
65. Chen, J., Burke, J. J., Xin, Z., Xu, C., and Velten, J. (2006) Characterization of the Arabidopsis thermosensitive mutant atts02 reveals important role of galactolipids in thermotolerance. *Plant Cell Environ.* **29,** 1437–1448 CrossRef Medline
66. Moellering, E. R., Muthan, B., and Benning, C. (2010) Freezing tolerance in plants requires lipid remodeling at the outer chloroplast membrane. *Science* **330,** 226–228 CrossRef Medline
67. Klecker, M., Gasch, P., Peisker, H., Dörmann, P., Schlicke, H., Grimm, B., and Mustroph, A. (2014) A shoot-specific hypoxic response of Arabidopsis sheds light on the role of the phosphate-responsive transcription factor PHOSPHATE STARVATION RESPONSE 1. *Plant Physiol.* **165,** 774–790 CrossRef Medline
68. Gasulla, F., vom Dorp, K., Dombrink, I., Zähringer, U., Gisch, N., Dörmann, P., and Bartels, D. (2013) The role of lipid metabolism in the acquisition of desiccation tolerance in *Craterostigma plantagineum*: A comparative approach. *Plant J.* **75,** 726–741 CrossRef Medline
69. Härtel, H., Dörmann, P., and Benning, C. (2000) DGD1-independent biosynthesis of extraplastidic galactolipids after phosphate deprivation in Arabidopsis. *Proc. Natl. Acad. Sci. U.S.A.* **97,** 10649–10654 CrossRef Medline
70. Burke, J. J., Ditto, C. L., and Arntzen, C. J. (1978) Involvement of the light-harvesting complex in cation regulation of excitation energy distribution in chloroplasts. *Arch. Biochem. Biophys.* **187,** 252–263 CrossRef Medline
71. Kühlbrandt, W., Thaler, T., and Wehrli, E. (1983) The structure of membrane crystals of the light-harvesting chlorophyll *a*/*b* protein complex. *J. Cell Biol.* **96,** 1414–1424 CrossRef Medline
72. Haferkamp, S., and Kirchhoff, H. (2008) Significance of molecular crowding in grana membranes of higher plants for light harvesting by photosystem II. *Photosyn. Res.* **95,** 129–134 CrossRef Medline
73. Kirchhoff, H., and Yarbrough, R. (2018) Evaluation of lipids for the study of photosynthetic membranes. *Methods Mol. Biol.* **1770,** 305–316 CrossRef Medline

Downloaded from http://www.jbc.org/ at Washington State University Libraries on March 24, 2020

ASBMB

A proteoliposome-based system reveals how lipids control photosynthetic light harvesting

Stefanie Tietz, Michelle Leuenberger, Ricarda Höhner, Alice H. Olson, Graham R. Fleming and Helmut Kirchhoff

J. Biol. Chem. 2020, 295:1857-1866.
doi: 10.1074/jbc.RA119.011707 originally published online January 12, 2020

Access the most updated version of this article at doi: 10.1074/jbc.RA119.011707

Alerts:
- When this article is cited
- When a correction for this article is posted

Click here to choose from all of JBC's e-mail alerts

This article cites 73 references, 15 of which can be accessed free at
http://www.jbc.org/content/295/7/1857.full.html#ref-list-1

Downloaded from http://www.jbc.org/ at Washington State University Libraries on March 24, 2020